

# Influence of Aluminum and Hydrogen on the Properties of $\text{Sm}_2\text{Fe}_{17}$

S. V. Veselova<sup>a, \*</sup>, V. N. Verbetsky<sup>a</sup>, A. G. Savchenko<sup>b</sup>, and I. V. Shchetinin<sup>b</sup>

<sup>a</sup>Faculty of Chemistry, Moscow State University, Moscow, Russia

<sup>b</sup>National University of Science and Technology MISiS, Moscow, Russia

\*e-mail: sv\_veselova@mail.ru

Received November 20, 2017

**Abstract**—Cast, homogenized, and hydrogenated alloys based on intermetallic compound  $\text{Sm}_2\text{Fe}_{17}$  with replacement of iron by aluminum to concentrations of 8.9, 17.9, 26.8, and 35.8 at % Al are investigated by the methods of X-ray fluorescence, X-ray diffraction analysis, and scanning electron microscopy. The alloys are hydrogenated at a temperature of 180°C and a pressure of 25–30 atm. It is established that all the hydrides of the nominal compositions  $\text{Sm}_2\text{Fe}_{14.9}\text{Al}_{2.1}\text{H}_{3.6}$ ,  $\text{Sm}_2\text{Fe}_{13.3}\text{Al}_{3.8}\text{H}_{2.1}$ ,  $\text{Sm}_2\text{Fe}_{10.7}\text{Al}_{6.3}\text{H}_2$ , and  $\text{Sm}_2\text{Fe}_{9.9}\text{Al}_{7.1}\text{H}_{1.8}$ , like  $\text{Sm}_2\text{Fe}_{17}$ , are crystallized in the rhombohedral  $\text{Th}_2\text{Zn}_{17}$  type of structure (space group  $R\bar{3}m$ ). The partial replacement of Fe in  $\text{Sm}_2\text{Fe}_{17}$  by Al is accompanied by a monotonic increase in the lattice periods and a simultaneous decrease in the specific saturation magnetization of the studied alloys. A similar trend is also established for the hydride phases.

**Keywords:** Sm–Fe–Al alloys, microstructural analysis, hydrogen, hydrides, crystal structure, magnetic properties

**DOI:** 10.1134/S2075113319010374

## INTRODUCTION

It is known that intermetallic compounds of rare-earth metals with a high content of iron, such as  $\text{R}_2\text{Fe}_{14}\text{B}$ ,  $\text{R}_2\text{Fe}_{17}$ , and  $\text{R}(\text{Fe}, \text{T})_{12}$  (T stands for Ti, Fe, Al, V, or Mo), possess enhanced magnetic properties and are of great practical interest owing to the high magnetocrystalline anisotropy shown by most of them; in particular, they are used in the production of powerful permanent magnets [1–3]. An analysis of the published data shows that the introduction of interstitial and substitutional atoms into the crystal lattice of compounds  $\text{R}_2\text{Fe}_{17}$  allows one to substantially change their properties—for example, Curie temperature  $T_C$  and the magnitude and behavior of the magnetocrystalline anisotropy—in consequence of changing the interatomic distances and the unit cell volume [4–8]. Light atoms contribute to modification of magnetic properties by changing the electronic structure of initial compounds, which is also determined by bulk effects (increases in the atomic volume and in the interatomic distances in R–Fe pairs and, particularly, in the Fe–Fe pair give rise to changes in the exchange interaction constants) accompanied by the enhancement of the magnetism of the iron sublattice and by the chemical effects upon incorporation of interstitial atoms.

The Nd–Fe–B hard magnetic alloys are a basis for the most powerful (in the climatic temperature range) permanent magnets. However, nitrides  $\text{Sm}_2\text{Fe}_{17}\text{N}_x$

( $x \leq 3$ ) discovered at the beginning of the 1990s can replace them in a number of very important applications in view of excellent magnetic characteristics ( $T_C$ , the saturation magnetization, and the anisotropy field value in them are higher than in neodymium magnets) and higher thermal stability (the thermal decomposition of this compound into the SmN and  $\alpha$ -Fe phases is observed at temperatures above 450°C) [9, 10]. In this regard, compound  $\text{Sm}_2\text{Fe}_{17}$  in which part of the samarium atoms are replaced by other rare-earth atoms and part of the iron atoms are replaced by non-magnetic elements is of considerable interest for study. For example, it was shown in [7, 11, 12] that the replacement of iron by Ga, Si, and Al gives rise to an increase in the  $T_C$  value and to the possibility of partial alteration of the sign of the magnetocrystalline anisotropy constant.

To date, quasibinary compounds  $\text{Sm}_2\text{Fe}_{17-x}\text{Al}_x$  have been studied in sufficient detail [7, 13–16]. In particular, it was established that these intermetallic compounds, like  $\text{Sm}_2\text{Fe}_{17}$ , have a rhombohedral structure of the  $\text{Th}_2\text{Zn}_{17}$  type. In addition, regularities regarding the magnetization/ $T_C$ –aluminum substitution level relationship were found in [14, 16]. For example, it was established that the Curie temperature first increases (when  $x \leq 3$ ) and then decreases rapidly with an increase in the concentration of aluminum. Substitution of aluminum also affects the magnetic anisotropy of  $\text{Sm}_2\text{Fe}_{17-x}\text{Al}_x$ . Thus, a low content of Al

( $x \leq 5$ ) in  $\text{Sm}_2\text{Fe}_{17}$  gives rise to the reorientation of the easy magnetization axis from the basal plane to the  $c$  axis, but its subsequent increase ( $5 \leq x \leq 7$ ) causes the reverse effect.

At the same time, the published data on the structure, phase composition, and magnetic properties of hydrides  $\text{Sm}_2(\text{Fe}, \text{Al})_{17}\text{H}_z$  are certainly insufficient, while the available information is fragmented. The lack of published data on the  $\text{Sm}-(\text{Fe}, \text{Al})-\text{H}$  system is probably caused by the fact that, in this case, as in the case of hydrides of  $\text{Sm}_2\text{Fe}_{17}$ , no radical changes in the magnetic properties are expected upon the incorporation of hydrogen atoms into the crystal lattice of the initial compound. For example, there is no information on the phase composition of the initial alloys with nominal composition  $\text{Sm}_2\text{Fe}_{17-x}\text{Al}_x$  ( $x = 0, 1, 2, 3$ ) in the study [17] devoted to the investigation of hydride phases in the  $\text{Sm}-(\text{Fe}, \text{Al})$  system. On the other hand, it has been established for the first time in this study that the Curie temperature values measured under heating conditions for hydrides based on  $\text{Sm}_2(\text{Fe}, \text{Al})_{17}$  are higher than the Curie temperature values measured upon cooling. The saturation magnetization values of the hydrides measured in a weak external magnetic field (0.04 T) at room temperature tend to decrease with an increase in the aluminum content at a simultaneous decrease in the  $\text{H}/\text{Sm}_2(\text{Fe}, \text{Al})_{17}$  ratio. In addition, one more tendency was revealed for hydrides  $\text{R}_2\text{Fe}_{17}\text{H}_y$  in the study, namely: the larger the change in the amount of absorbed hydrogen in the compound, the poorer the stability of the hydride, and vice versa. The authors claim that the stability of hydrides of compounds  $\text{Sm}_2(\text{Fe}, \text{Al})_{17}$  decreases with an increase in the concentration of aluminum.

In the present work, the influence of the content of aluminum and hydrogen on the structure and magnetic properties (specific saturation magnetization  $\sigma_s$  and magnetization coercive force  $jH_c$ ) of homogenized alloys of the  $\text{Sm}-\text{Fe}-\text{Al}$  system and hydrides of relevant quasibinary compounds  $\text{Sm}_2(\text{Fe}, \text{Al})_{17}$  is studied. The obtained results complement and expand the existing published data on hydrides based on the  $\text{Sm}-\text{Fe}-\text{Al}$  alloys.

## EXPERIMENTAL

Alloys based on intermetallic compound  $\text{Sm}_2\text{Fe}_{17}$  with aluminum contents of 8.9, 17.9, 26.8, and 35.8 at % (the planned composition was  $\text{Sm}_2(\text{Fe}_{1-x}\text{Al}_x)_{17}$ ,  $x = 0.1, 0.2, 0.3, 0.4$ ) for studies were obtained in electric arc and induction ( $x = 0.4$ ) furnaces by fusing the batch mixture of high-purity metals (the purity of Sm was 99.5%, the purity of Fe was 99.9%, and the purity of Al was 99.99%) in an atmosphere of purified argon. To compensate for the burning loss of samarium, its actual content in the charge during the smelting was higher than the theoretical value by 5%. The obtained ingots were subjected to homogenizing annealing at a

temperature of 1000°C for 40 h in evacuated quartz vials in order to obtain a uniform microstructure. The compositions of the alloys after homogenization and their microstructure were controlled by the methods of X-ray diffraction (XRD) and chemical (elemental) analyses, and scanning electron microscopy.

Alloys and hydrides based on them were studied by the X-ray diffraction method on a DRON-4-07 diffractometer ( $U = 40$  kV,  $I = 30$  mA) using monochromatic  $\text{CoK}\alpha$  radiation by point-by-point scanning with increments of 0.05 degrees within the range  $2\theta = 20^\circ - 120^\circ$  and exposure for 5 s per each point of recording. The Rietan-2000 software package was used to determine the crystal lattice parameters of the initial alloys and their hydride phases by the Rietveld method. The accuracy in determining the lattice periods was  $\pm(0.01-0.05\%)$  and in establishing the mass ratio of phases was  $\pm(5-10\%)$ . The chemical compositions of cast samples were determined using the method of X-ray fluorescence analysis on a Rigaku Primus II wavelength dispersive spectrometer. Electron-microscopic studies were carried out on TESCAN VEGA 3 SBH and LEO EVO 50 XVP microscopes equipped with an attachment for energy-dispersive analysis. The error in determining the concentration of elements did not exceed 0.5 at %.

The investigated alloys (samples with a weight of 9–11 g) were hydrogenated in a special facility designed for this purpose by the direct reaction of the initial alloys with high-purity hydrogen (the content of impurities was  $10^{-3}-10^{-4}$  wt %) obtained by desorption from a hydride phase based on intermetallic compound  $\text{LaNi}_5$ . It was established that the interaction of the investigated alloys with hydrogen is observed only after heating to 200°C under a pressure of 25–30 atm. The amount of absorbed hydrogen was determined on the basis of a difference in the gas pressure before and after the reaction, and the compositions of derived hydrides were calculated using the van der Waals equation. The relative error in determining the hydrogen content was  $\pm 0.1$  H/ $\text{Sm}_2(\text{Fe}, \text{Al})_{17}$  ( $\pm 0.05$  wt %  $\text{H}_2$ ).

The magnetic measurements were carried out at room temperature in magnetic fields of up to 9 T using a magnetic vibrator attached to a PPMS-9 Ever Cool II measuring system. To measure the  $\sigma_s$  and  $jH_c$  values, powder samples with a weight of 10–15 mg were poured into plastic cylindrical hollow cuvettes, covered with melted paraffin, and reinforced with a cap. The accuracy of measuring the magnetization was  $\pm 2$  A m<sup>2</sup> kg<sup>-1</sup>.

## RESULTS AND DISCUSSION

### *Characteristics of Initial Alloys $\text{Sm}_2(\text{Fe}_{1-x}\text{Al}_x)_{17}$ : Chemical (Elemental) and Phase Compositions*

The results of X-ray fluorescence, energy-dispersive, and X-ray diffraction analyses of the cast alloys (Table 1) showed that all synthesized samples are inhomogeneous and contain primary precipitates of

**Table 1.** Calculated compositions, the results of X-ray fluorescence analysis, and the phase compositions of cast\*\*  $\text{Sm}_2(\text{Fe}_{1-x}\text{Al}_x)_{17}$  alloy samples

Nominal composition	Calculated contents of components, wt (at*) %			Results of X-ray fluorescence analysis, wt %			Phase composition (according to data of XRD analysis and energy dispersive microanalysis)
	Sm	Fe	Al	Sm	Fe	Al	
(1) $\text{Sm}_2\text{Fe}_{15.3}\text{Al}_{1.7}$	25.04 (10.5)	71.15 (80.5)	3.82 (8.9)	20.73	75.07	3.18	$\text{Sm}_2(\text{Fe}, \text{Al})_{17}$ $\alpha\text{-Fe}(\text{Al})$ $\text{Sm}(\text{Fe}, \text{Al})_3$
(2) $\text{Sm}_2\text{Fe}_{13.6}\text{Al}_{3.4}$	26.1 (10.5)	65.93 (71.6)	7.96 (17.9)	23.21	70.48	5.26	$\text{Sm}_2(\text{Fe}, \text{Al})_{17}$ $\alpha\text{-Fe}(\text{Al})$ $\text{Sm}(\text{Fe}, \text{Al})_3$ (traces)
(3) $\text{Sm}_2\text{Fe}_{11.9}\text{Al}_{5.1}$	27.26 (10.5)	60.26 (62.6)	12.48 (26.8)	23.86	64.3	10.82	$\text{Sm}_2(\text{Fe}, \text{Al})_{17}$ $\alpha\text{-Fe}(\text{Al})$
(4) $\text{Sm}_2\text{Fe}_{10.2}\text{Al}_{6.8}$	28.53 (10.5)	54.06 (53.7)	17.41 (35.8)	28.67	54.53	16.7	$\text{Sm}_2(\text{Fe}, \text{Al})_{17}$ $\alpha\text{-Fe}(\text{Al})$ $\text{Sm}(\text{Fe}, \text{Al})_3$ (traces)

\* The calculated contents of elements in atomic percentages are given in parentheses.

\*\* Cast alloys 1, 2, and 3 were obtained in a vacuum arc furnace and alloy 4 was obtained by the method of vacuum induction melting.

$\alpha\text{-Fe}$  and  $\text{Sm}_2(\text{Fe}_{1-x}\text{Al}_x)_{17}$  and also the phases enriched in samarium. Typical microstructures of samples before (1, 2, 3, and 4) and after (1a, 2a, 3a, and 4a) the homogenizing annealing are shown in Fig. 1.

As is known, the formation of a homogeneous structure and the 2:17 phase as a result of the reaction between the phase enriched in samarium and crystalline  $\alpha\text{-Fe}$  is achieved by high-temperature homogenization. As was noted in [18], the partial replacement of iron by silicon or aluminum in combination with some redundant content of samarium in compounds of the  $\text{Sm}_2(\text{Fe}, \text{M})_{17}$  type gives rise to the effective suppression of precipitates of  $\alpha\text{-Fe}$  during the annealing. However, the mentioned effect was not observed in our alloys. According to the results of SEM and XRD analysis, we obtained binary alloys—the studied  $\text{Sm}_2(\text{Fe}_{1-x}\text{Al}_x)_{17}$  samples contain a significant amount of the impurity phase based on  $\alpha\text{-Fe}$  in addition to the main phase possessing the structure of the  $\text{Th}_2\text{Zn}_{17}$  type, space group  $R\bar{3}m$  (Table 2). X-ray diffraction patterns of the studied alloys after the homogenizing annealing are illustrated in Fig. 2. As can be seen from the results given in Table 1, this is determined by the fact that samarium evaporates very quickly in the process of smelting by the electric arc method (unlike the induction method) and an excess of 5% samarium taken to compensate the burning loss is certainly insufficient. As a result, the content of the soft magnetic phase in samples can reach 43 wt %.

#### *Structure and Magnetic Properties of the $\text{Sm}_2(\text{Fe}, \text{Al})_{17}$ Phases and Products of Their Hydrogenation*

Just before beginning the hydrogenation procedure, the starting materials were thoroughly crushed,

because otherwise, as shown by the results of preliminary experiments, a high content of the  $\alpha\text{-Fe}(\text{Al})$  phase impedes the completion of the reaction of  $\text{Sm}_2(\text{Fe}, \text{Al})_{17}$  with hydrogen (the  $\alpha\text{-Fe}$  phase is not hydrogenated). Therefore, reflections of the initial phase uninvolved in the reaction with hydrogen were also present in the X-ray diffraction patterns of the hydrogenated alloys.

Given that none of synthesized samples interacted with hydrogen at room temperature, hydrogenation was carried out by heating to 200°C under a hydrogen pressure of 25–30 atm. The amount of absorbed hydrogen was brought into correlation with the amount of the  $\text{Sm}_2(\text{Fe}, \text{Al})_{17}$  phase in the initial alloy. On the basis of the XRD analysis, a slight decrease in the intensity of the peaks of the  $\alpha\text{-Fe}(\text{Al})$  phase was observed in the X-ray diffraction patterns of alloys  $\text{Sm}_2(\text{Fe}, \text{Al})_{17}\text{H}_y$ ,  $y = 1.8\text{--}3.6$ , while the intensity of the lines of the main phase did not change, and only their broadening caused by the incorporation of hydrogen atoms into the crystal lattice of intermetallic compounds  $\text{Sm}_2(\text{Fe}, \text{Al})_{17}$  was noticed.

The results of structural and magnetic measurements of all samples synthesized in the present work with consideration that the indicated values were recalculated to wt % of the 2 : 17 phase and their comparison with the published data are given in Table 2. Moreover, the indicated values of specific saturation magnetization  $\sigma_s(2 : 17)$  in a field of 7.164 MA/m were calculated according to the following formula:

$$\sigma_s(2 : 17) = \sigma_s(\text{sample}) - \sigma_s(\alpha\text{-Fe})\omega(\alpha\text{-Fe}, \text{Al})/\omega(2 : 17), \quad (1)$$

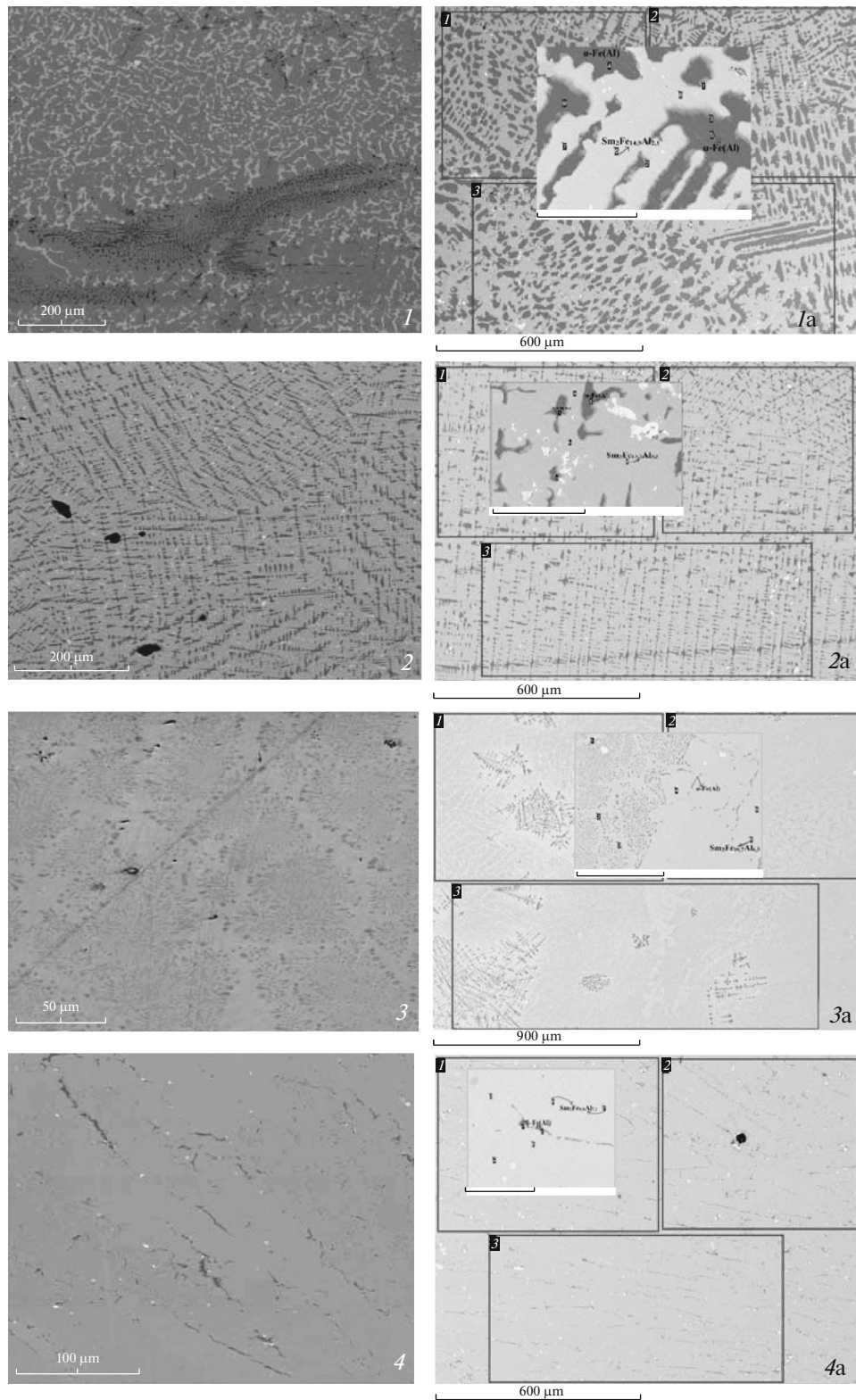


**Fig. 1.** Microstructures of the cast (samples 1, 2, 3, and 4; on the left) alloys and the alloys homogenized for 40 h at 1000°C (samples 1a, 2a, 3a, and 4a; on the right). The cast alloys: (1) sample no. 1 containing  $\alpha$ -Fe(Al) (black) in addition to the main 2 : 17 phase (dark gray) surrounded by  $\text{Sm}(\text{Fe}, \text{Al})_3$  (gray); (2) sample no. 2 with the predominant 2 : 17 phase surrounded by  $\alpha$ -Fe(Al) with traces of  $\text{Sm}(\text{Fe}, \text{Al})_3$ ; (3) sample no. 3 with a high content of  $\alpha$ -Fe(Al) in addition to the main 2 : 17 phase; (4) sample no. 4 with the predominant 2 : 17 phase, a low concentration of  $\alpha$ -Fe(Al), and an insignificant concentration of  $\text{Sm}(\text{Fe}, \text{Al})_3$ . The homogenized alloys: (1a) sample no. 1a composed of  $\text{Sm}_2\text{Fe}_{14.9}\text{Al}_{2.1}$  and  $\alpha$ -Fe(Al); (2a) sample no. 2a composed of  $\text{Sm}_2\text{Fe}_{13.2}\text{Al}_{3.8}$  and  $\alpha$ -Fe(Al); (3a) sample no. 3a composed of  $\text{Sm}_2\text{Fe}_{10.7}\text{Al}_{6.3}$  and  $\alpha$ -Fe(Al); (4a) sample no. 4a composed of  $\text{Sm}_2\text{Fe}_{9.9}\text{Al}_{7.1}$  and  $\alpha$ -Fe(Al). The  $\text{Sm}_2(\text{Fe}, \text{Al})_{17}$  phase is gray and the  $\alpha$ -Fe(Al) phase is black; the defects of polishing are highlighted in white.

**Table 2.** X-ray diffraction and magnetic characteristics of the 2 : 17 phases and their hydrogenation products (structure type  $\text{Th}_2\text{Zn}_{17}$ ; space group  $R\bar{3}m$ ; no. 166) compared to the published data [17]

Composition of the 2 : 17 phase in the initial sample and the hydrogenation products	Content of the 2 : 17 phase, wt %	$a$ , Å	$c$ , Å	$c/a$	$V$ , Å <sup>3</sup>	$\Delta V/V_0$ , %	$\sigma_s^*$ , A m <sup>2</sup> /kg
$\text{Sm}_2\text{Fe}_{16}\text{Al}$ [17]	Not specified	8.577	12.503	1.201	796.7	3	112.3
$\text{Sm}_2\text{Fe}_{16}\text{AlH}_{3.1}$ [17]		8.680	12.578	1.449	820.8		139.1
$\text{Sm}_2\text{Fe}_{15}\text{Al}_2$ [17]	Not specified	8.612	12.538	1.456	805.2		103.6
$\text{Sm}_2\text{Fe}_{15}\text{Al}_2\text{H}_{2.8}$ [17]		8.698	12.600	1.449	825.5	2.5	137.4
$\text{Sm}_2\text{Fe}_{14.9}\text{Al}_{2.1}$	57	8.603 (4)	12.522 (3)	1.456	802.7		95.9
$\text{Sm}_2\text{Fe}_{14.9}\text{Al}_{2.1}\text{H}_{3.6}$		8.698 (1)	12.655 (3)	1.455	827.3	~3	97.5
$\text{Sm}_2\text{Fe}_{14}\text{Al}_3$ [17]	Not specified	8.635	12.548	1.453	810.3		95.4
$\text{Sm}_2\text{Fe}_{14}\text{Al}_3\text{H}_{2.6}$ [17]		8.704	12.598	1.447	826.6	2	123.3
$\text{Sm}_2\text{Fe}_{13.3}\text{Al}_{3.8}$	72	8.643 (7)	12.596 (3)	1.457	815.6		69.6
$\text{Sm}_2\text{Fe}_{13.3}\text{Al}_{3.8}\text{H}_{2.1}$		8.700 (2)	12.684 (9)	1.458	831.6	2	83.5
$\text{Sm}_2\text{Fe}_{10.7}\text{Al}_{6.3}$	75	8.695 (3)	12.670 (5)	1.457	829.9		62.4
$\text{Sm}_2\text{Fe}_{10.7}\text{Al}_{6.3}\text{H}_2$		8.750 (2)	12.763 (2)	1.459	846.1	1.9	64.1
$\text{Sm}_2\text{Fe}_{9.9}\text{Al}_{7.1}$	96	8.759 (0)	12.740 (4)	1.454	846.5		22.1
$\text{Sm}_2\text{Fe}_{9.9}\text{Al}_{7.1}\text{H}_{1.8}$		8.799 (3)	12.813 (6)	1.456	859.2	1.5	32.9

\* The  $\sigma_s$  values of the present study were calculated by Eq. (1).

where the used value  $\sigma_s(\alpha\text{-Fe}) = 210 \text{ A m}^2/\text{kg}$  was measured at room temperature [19], and  $\omega$  is the content of the phase in the sample, wt %.

The amounts of hydrogen absorbed by the 2 : 17 phase obtained in our work and in [17] are different.

Namely, they are slightly higher in the former case as compared to the published data, so the observed values of saturation magnetization are smaller than those reported in the literature source. It can be assumed that the preliminary grinding of the starting material

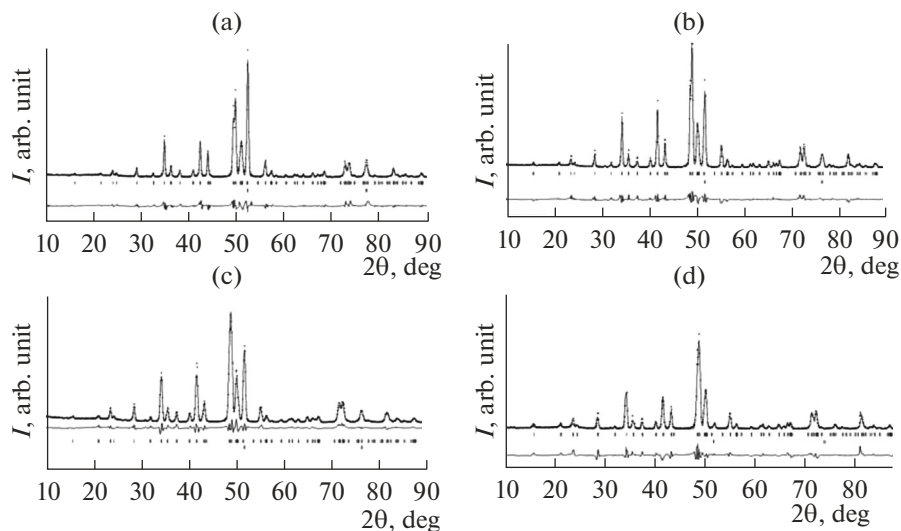


**Fig. 2.** X-ray diffraction patterns of the Sm–Fe–Al alloy samples after annealing at 1000°C for 40 h: (a) no. 1a, (b) no. 2a, (c) no. 3a, and (d) no. 4a. The experimental data are shown by dots, the calculated data by lines, and the  $hkl$  reflections by strokes; the bottom line shows the difference between the experimental and calculated data. The upper series of strokes corresponds to the main  $\text{Sm}_2(\text{Fe}_{1-x}\text{Al}_x)_{17}$  phase and the lower series of strokes corresponds to the impurity  $\alpha$ -(Fe, Al) phase.

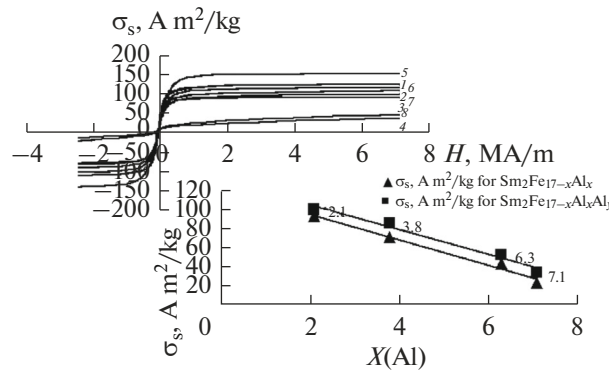


**Fig. 3.** Magnetic hysteresis loops measured at room temperature for samples 1a, 2a, 3a, and 4a (curves 1–4), and their hydrogenation products (curves 5–8), respectively. The concentration dependence of specific magnetization  $\sigma_s$  for these compounds in a magnetic field of 7.164 MA/m is shown in the inset.

gave rise to the more efficient hydrogenation process and we have higher parameters relative to  $H/\text{Sm}_2(\text{Fe}, \text{Al})_{17}$  as a result.

According to the analysis of the X-ray diffraction patterns of the obtained hydrides, incorporation of hydrogen atoms is accompanied by an increase in the unit cell volume of the initial 2 : 17 phase without changing its structural type as in the case of hydrides  $\text{Sm}_2\text{Fe}_{17}\text{H}_k$  ( $k = 2-5.5$ ) studied in detail in the literature.

The value of volume change  $\Delta V/V_0$  for the hydrogenated 2 : 17 phase varies in the range from about 3 to 1.5% with respect to this phase in the initial alloys. It should be noted that  $(\Delta V/V_0)/H$  and lattice parameters  $a$  and  $c$  of  $\text{Sm}_2(\text{Fe}_{1-x}\text{Al}_x)_{17}\text{H}_y$  monotonically decrease with an increase in the aluminum content. On the whole, the effect of expanding the lattice volume shows a decreasing behavior not only because of the replacement of iron atoms by larger aluminum atoms but also on account of a decrease in the amount of absorbed hydrogen in the hydride phases with an increase in the concentration of aluminum. Neglecting a relatively small discrepancy associated with the experimental error, one can assert that the  $c/a$  ratio barely depends on the concentration of aluminum in both the initial phase and hydrogenation products, which points to the fact that the increase in the lattice parameters is basically an isotropic process. In addition, as follows from the obtained results (see Table 2), changing the aluminum content has an effect on the value of hydrogen absorption in the alloys, which decreases as expected. Therefore, perhaps it would be more correct to call hydrogenation products  $\text{Sm}_2(\text{Fe}, \text{Al})_{17}\text{H}_y$  ( $y = 1.8-3.6$ ) “solid solutions of hydrogen in  $\text{Sm}_2(\text{Fe}, \text{Al})_{17}$ ” rather than “hydrides.”

The magnetic hysteresis loops of samples of cast homogenized alloys  $\text{Sm}_2\text{Fe}_{17-x}\text{Al}_x$  and their hydrogenation products measured at room temperature in magnetic fields with strengths ranging from  $-7.164$  to

$+7.164$  MA/m, which show that the introduction of hydrogen leads to an increase in the  $\sigma_s$  value (the specific magnetization in the field is 7.164 MA/m) compared to the initial alloys, are given in Fig. 3. However, the degree of this increase dramatically decreases with an increase in the concentration of aluminum, and as a result, the value of specific magnetization  $\sigma_s$  in both the cast homogenized and hydrogenated  $\text{Sm}_2\text{Fe}_{17-x}\text{Al}_x$  alloys generally tends to decrease monotonically. It should be noted that this decrease occurs much faster than in the case of simple “magnetic dilution.”

According to the hysteresis curves given in Figs. 4a–4h, the introduction of hydrogen into Sm–Fe–Al alloys has a weak effect on the coercive force, which retains values that are close to zero in the  $\text{Sm}_2(\text{Fe}, \text{Al})_{17}\text{H}_y$  samples, which is primarily due to the presence of the magnetocrystalline anisotropy of the “easy plane” type and also due to the replacement of iron atoms by nonmagnetic aluminum atoms that weaken the manifestation of ferromagnetic properties by the compounds when hydrogen is incorporated into the crystal lattice of the initial alloy. Hence, these hydrogenation products can be regarded as belonging to the class of typical soft magnetic materials.

Thus, it can be concluded on the basis of structural and magnetic measurements that the replacement of iron by aluminum reduces, in general, the solubility of hydrogen in pseudobinary compound  $\text{Sm}_2(\text{Fe}_{1-x}\text{Al}_x)_2$ , which leads to decreases in the amount of hydrogen absorbed by the material, the  $(\Delta V/V_0)/H$  ratio, and specific magnetization  $\sigma_s$  in a magnetic field of 7.164 MA/m.

### CONCLUSIONS

In the present work, the alloys that are close in composition to the stoichiometry of intermetallic compound  $\text{Sm}_2\text{Fe}_{17}$  (2 : 17), containing 8.9, 17.9, 26.8, and 35.8 at % of aluminum, have been investigated. The main 2 : 17 phase (>50 wt %) has a crystal struc-

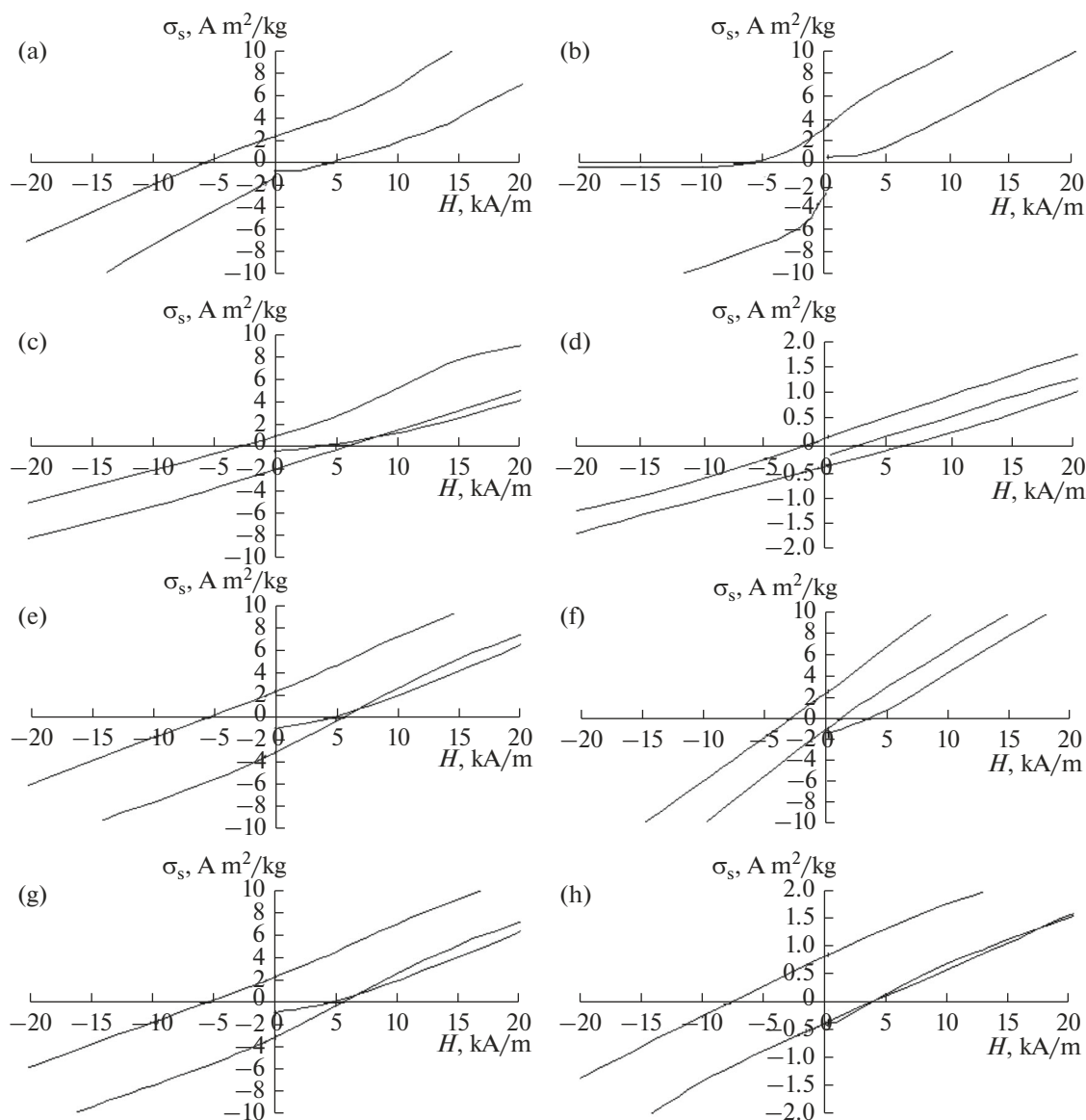


**Fig. 4.** Fragments of hysteresis loops in the vicinity of the coordinate system origin, which were used to assess the coercive force of the initial homogenized alloy samples (a) 1a, (b) 2a, (c) 3a, and (d) 4a, and (e–h) their hydrogenation products, respectively.

ture of the  $\text{Th}_2\text{Zn}_{17}$  type (space group  $R\bar{3}m$ ). As a result of the reaction of powders of the cast homogenized alloys with hydrogen, hydride phases of nominal composition  $\text{Sm}_2\text{Fe}_{17-x}\text{Al}_x\text{H}_y$ , where  $x = 2.1, 3.8, 6.3,$  and  $7.1$  and  $y = 3.6, 2.1, 1.8,$  and  $2$ , respectively, with a crystalline structure relating to the same  $\text{Th}_2\text{Zn}_{17}$  structural type are obtained.

The replacement of iron by aluminum in  $\text{Sm}_2\text{Fe}_{17}$  increases the unit cell volume and the introduction of hydrogen contributes to the additional increase in the lattice parameters. However, the amount of absorbed hydrogen and relative expansion  $\Delta V/V_0$  of the unit cell volume decrease with an increase in the concentration of aluminum in the 2 : 17 phase, which indicates,

together with an analysis of the magnetic hysteresis loops of the Sm–Fe–Al powders and hydride phases based on them, that the replacement of iron by aluminum reduces the solubility of hydrogen in pseudobinary compound  $\text{Sm}_2(\text{Fe}, \text{Al})_{17}$ . In addition, the obtained results suggest that hydrogenation products  $\text{Sm}_2(\text{Fe}, \text{Al})_{17}\text{H}_y$  ( $y = 1.8–3.6$ ) are solid solutions of hydrogen in  $\text{Sm}_2(\text{Fe}, \text{Al})_{17}$ .

## REFERENCES

1. Hirosawa, S., Nishino, M., and Miyashita, S., Perspectives for high-performance permanent magnets: applications, coercivity, and new materials, *Adv. Nat. Sci.*

- Nanosci. Nanotechnol.*, 2017, vol. 8, art. ID 013002. doi 10.1088/2043-6254/aa597c
2. Fang, Q., An, X., Wang, F., Li, Y., Du, J., Xia, W., Yan, A., Liu, J.P., and Zhang, J., The structure and magnetic properties of Sm–Fe–N powders prepared by ball milling at low temperature, *J. Magn. Magn. Mater.*, 2016, vol. 410, pp. 116–122. doi 10.1016/j.jmmm.2016.03.029
  3. Anikina, E.Yu., Verbetskiy, V.N., Savchenko, A.G., Menushenkov, V.P., and Shchetinin, I.V., Investigation of hydrogen interaction with magnetic materials of Nd–Fe–B type by calorimetry method, *Inorg. Mater.: Appl. Res.*, 2016, vol. 7, no. 4, pp. 497–501.
  4. Gudin, S.A., Isupova, N.N., and Tereshina, I.S., Physical mechanisms of Curie temperature measurement in compounds  $R_2Fe_{17}$  (R–rare Earth) during implementation of nonmagnetic atoms C, N, H, *Gorn. Inf.-Anal. Byull.*, 2007, suppl. 1, pp. 360–374.
  5. Pastushenkov, Yu.G., Skokov, K.P., Lyakhova, M.B., and Antonova, E.S., Domain structure of  $R_2Fe_{17}$  intermetallic compounds with planar-type anisotropy, *J. Met. Sci. Heat Treat.*, 2017, vol. 58, pp. 594–598. doi 10.1007/s11041-017-0061-9
  6. Isnard, O., Miraglia, S., and Fruchart, D., Interstitial insertion in  $R_2Fe_{17}$ , volume effects and their correlation with the magnetic properties, *J. Magn. Magn. Mater.*, 1995, vol. 144, pp. 981–982. (94) 01458-2 doi 10.1016/0304-8853
  7. Rama Rao, K.V.S., Ehrenberg, H., Markandeyulu, G., Varadaraju, U.V., Venkatesan, M., Suresh, K.G., Murthy, V.S., Schmidt, P.C., and Fuess, H., On the structural and magnetic properties of  $R_2Fe_{17-x}(A, T)_x$  (R = rare earth; A = Al, Si, Ga; T = transition metal) compounds, *Phys. Status Solidi A*, 2002, vol. 189, no. 2, pp. 373–388. 2-G doi 10.1002/1521-396X(200202)189:2<373::AID-PSSA373>3.0.CO
  8. Tereshina, I.S., Nikitin, S.A., Verbetskiy, V.N., and Salamova, A.A., Transformations of magnetic phase diagram as a result of insertion of hydrogen and nitrogen atoms in the crystalline lattice of  $R_2Fe_{17}$  compounds, *J. Alloys Compd.*, 2002, vol. 336, nos. 1–2, pp. 36–40. (01) 01871-0 doi 10.1016/S0925-8388
  9. Sun, H., Coey, J.M.D., Otami, Y., and Hurley, D.P.F., Magnetic properties of a new series of rare-earth iron nitrides:  $R_2Fe_{17}N_y$  (y approximately 2.6), *J. Phys.: Condens. Matter*, 1990, vol. 2, pp. 6465–6470. doi 10.1088/0953-8984/2/30/013
  10. Otani, Y., Hurley, D.P.F., Hong, S., and Coey, J.M.D., Magnetic properties of a new family of ternary rare-earth iron nitrides  $R_2Fe_{17}N_{3-8}$  (invited), *J. Appl. Phys.*, 1991, vol. 69, no. 8, pp. 5584–5589. doi 10.1063/1.347957
  11. Zarek, W., Influence of Si, Al and C on the crystal structure and magnetic properties of  $Sm_2Fe_{17}$ , *J. Magn. Magn. Mater.*, 1996, vols. 157–158, pp. 91–92. doi 10.1016/0304-8853(95)01079-3
  12. Maruyama, F., Magnetic properties of  $Y_2Fe_{17-x}Ga_x$  and  $Sm_2Fe_{17-x}Ga_x$  compounds, *J. Mater. Sci.*, 2005, vol. 40, pp. 6517–6521. doi 10.1007/s10853-005-1600-0
  13. Wu, C.H., Ge, W.Q., Jin, X.M., Zhou, G.F., Chuang, Y.C., Zhu, Y.X., and Boer, F.R., Structure, magnetization and magnetostriction of  $Sm_2Fe_{17-x}Al_x$  compounds, 1993, vol. 202, pp. 129–132. (93) 90530-Z doi 10.1016/0925-8388
  14. Wang, Z. and Dunlap, R.A., Effects of Al substitutions on the magnetic properties of  $Sm_2Fe_{17}$  compounds, *J. Phys.: Condens. Matter*, 1993, vol. 5, pp. 2407–2414. doi 10.1088/0953-8984/5/15/011
  15. Al-Omari, I.A., Jaswal, S.S., Fernando, A.S., and Sellmyer, D.J., Mössbauer study of permanent-magnet materials:  $Sm_2Fe_{17-x}Al_x$  compounds, *J. Appl. Phys.*, 1994, vol. 76, no. 10, pp. 6159–6161. doi 10.1063/1.358340
  16. Cheng, Z., Shen, B., Liang, B., Zhang, J., Wang, F., Zhang, S., and Gong, H., The change in magnetic anisotropy in  $R_2Fe_{17-x}Al_x$  compounds (R = Sm or Tb), *J. Phys.: Condens. Matter*, 1995, vol. 7, pp. 4707–4712. doi 10.1088/0953-8984/7/24/010
  17. Rengen, X., Xinhua, W., Jianmin, W., Hongge, P., Changpin, C., Qidong, W., and Lichi, D., Effects of Al content on structural stability and magnetic properties of  $Sm_2(Fe, Al)_{17}$  compounds, *J. Trans. Nonferrous Met. Soc. China*, 1999, vol. 9, no. 1, pp. 40–43.
  18. Kubis, M., Gutfleisch, O., Gebel, B., Muller, K.-H., Harris, I.R., and Schultz, L., Influence of M = Al, Ga and Si on microstructure and HDDR-processing of  $Sm_2(Fe, M)_{17}$  and magnetic properties of their nitrides and carbides, *J. Alloys Compd.*, 1999, vol. 283, pp. 296–303. doi 10.1016/S0925-8388(98)00861-5
  19. Coey, J.M.D., *Magnetism and Magnetic Materials*, Cambridge: Cambridge Univ. Press, 2010. doi 10.1080/00107514.2010.514061

Translated by O. Kadkin